J. Phys.: Condens. Matter 4 (1992) 535–544. Printed in the UK

Photoluminescence of exchange-coupled Mo^{3+} pairs in $CsMgCl_3$

K Marney†, A H Francis†, G L McPherson‡ and P J McCarthy§

† Department of Chemistry, University of Michigan, Ann Arbor, MI 48109, USA
‡ Department of Chemistry, Tulane University, New Orleans, LA 70118, USA
§ Department of Chemistry, Canisius College, Buffalo, NY 14208, USA

Received 5 June 1991

Abstract. The high-resolution luminescence spectra of $CsMgCl_3$ doped with Mo^{3+} contain bands that are very temperature-sensitive between 5 K and 2 K and that can be assigned to exchange-coupled Mo^{3+}–V–Mo^{3+} pair centres (V = divalent vacancy). When the host lattice is doped with *both* Mo^{3+} and Li^+ it is found that pair formation is inhibited and the spectra are principally those of the single Mo^{3+} cation. Well-resolved multi-line luminescence spectra have been obtained from exchange-coupled Mo^{3+} pairs in the far red and near infrared. The spectra correlate well with the reported ground-state energy levels of the pairs as calcualed from EPR measurements.

1. Introduction

The luminescence from materials containing trivalent chromium has been studied extensively over the past fifty years. As part of the general interest in this area, the spectroscopic properties of dimeric systems containing magnetically coupled Cr^{3+} ions have been examined in considerable detail. In contrast, the luminescence from trivalent molybdenum, the second row analogue of Cr^{3+}, has not been nearly so well studied. The investigation of Flint and Paulusz [1] represents one of the few detailed analyses of the emissions from materials containing Mo^{3+}. That study, however, focused on monomeric complexes. The behaviour of coupled Mo^{3+} pairs has received very little attention. It was noted in a preliminary communication that crystals of $CsMgCl_3$ and $CsCdBr_3$ doped with Mo^{3+} luminesce strongly when excited in the visible region [2]. These salts adopt the linear-chain $CsNiCl_3$ structure in which the octahedral MX_6^{4-} groups share opposite faces to form infinite $[MX_3^-]_n$ chains with the Cs^+ ions positioned between the chains [3].

Electron paramagnetic resonance (EPR) studies indicate that the incorporation of trivalent molybdenum, or other trivalent ions, into the linear-chain lattice is primarily controlled by local charge compensation requirements [4–6]. While local charge neutrality can be achieved by a number of arrangements of dopant cations and lattice vacancies, one dimeric centre dominates. This centre consists of two trivalent ions located in the $[MX_3^-]_n$ chain on either side of a divalent cation vacancy (V). The linear Mo^{3+}–V–Mo^{3+} centre is illustrated in figure 1. The tendency to form this centre makes the $CsMX_3$ salts ideal host materials for the study of magnetically

0953-8984/92/020535+10$03.50

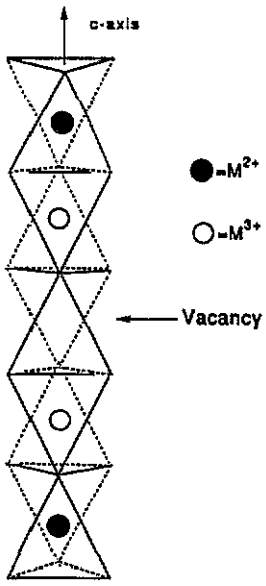

Figure 1. Structure of the Mo–V–Mo pair centre. Halide ions occupy the corners of the octahedra.

coupled pairs. Relatively small amounts of other types of trivalent ion centres (e.g. Mo^{3+}–Mo^{3+}–V) may also be present in the crystals.

Co-doping the lattice with small monovalent cations such as Li^+ offers an alternative mechanism by which charge compensation can be achieved. The trivalent ion may enter a $[MX_3^-]_n$ chain in conjunction with a lithium cation to give an Mo^{3+}–Li^+ centre. Thus, Li^+ co-doping can be used to suppress dimer formation.

$CsMgCl_3$ crystals containing Mo^{3+} luminesce strongly in the far red and near infrared when excited in the visible between 400 and 500 nm. The structured, sharp-line luminescence spectrum in the 710 to 730 nm region has been assigned to emission from the $^2T_2$ state of the Mo^{3+} ion and the associated dimer states. A second sharp luminescence in the 1100 to 1160 nm region can be attributed to the ^2E excited state. Unlike lanthanide ions, multiple state emission such as this is relatively rare for transition metal ions.

In principle, optical spectroscopy permits observation of the entire ground state manifold of dimer states. If the emission or absorption spectra of a magnetically coupled dimer centre can be sufficiently well resolved, it is possible to observe directly the exchange splittings in both the ground and excited states. The Mo^{3+}–V–Mo^{3+} exchange coupling has been examined previously by EPR spectroscopy. At X-band and Q-band frequencies, EPR can directly observe only a small portion of the ground state dimer manifold. Nevertheless, values of the magnetic interaction parameters for the entire manifold can be extracted from a theoretical fit to the observed EPR spectrum [4].

In the present paper, we have undertaken an investigation of the sharp-line photoluminescence spectra of Mo^{3+}-doped $CsMgCl_3$ under high resolution at low temperatures to determine if the exchange splittings in the Mo^{3+}–V–Mo^{3+} centres could be observed and analysed directly. We have obtained the ground state manifold splitting from photoluminescence spectra and compared these observations with theory using

the parameters derived from EPR studies.

2. Experimental procedure

2.1. Sample preparation

The synthesis of the molybdenum-doped crystals has been previously described [3]. The lithium-compensated crystals were prepared in a similar manner, by addition of equimolar amounts of the molybdenum chloride and lithium chloride. Due to the partitioning of impurities between the solid and melt during growth, the final crystal stoichiometry does not reflect the initial relative amounts of molybdenum and lithium. Chemical microanalysis of the crystals for molybdenum and lithium yielded the following compositions:

$$\begin{aligned} &(\text{ClMo}) && CsMgCl_3(Mo^{3+})_{0.006} \\ &(\text{ClMoLi}) && CsMgCl_3(Mo^{3+})_{0.002}(Li^{+})_{0.03}. \end{aligned}$$

The shorthand notation indicated in brackets is used throughout the text. It should be noted that the ClMoLi sample contained excess lithium beyond that necessary to compensate the molybdenum present. The principal use of the lithium-compensated crystals, in which dimer formation is suppressed, is to identify the dimer emission observed from the uncompensated samples.

2.2. Spectroscopic measurements

The crystals were cooled using a Janis 10DT liquid helium cryostat. Spectra were recorded at about 5 K by placing the crystal in thermal contact with normal boiling helium. Spectra at about 2 K were recorded with the crystal immersed in superfluid liquid helium.

Photoluminescence was excited with the 457 nm line of a 5 watt Coherent Innova 90 argon ion laser. The luminescence was passed through a Corning 3-71 glass filter to remove scattered laser radiation, dispersed with a 1 m scanning monochromator and detected with a cooled, red-sensitive, Hamamatsu R1767 photomultiplier tube. Absorption spectra were recorded in a single beam configuration using the broad-band output from a 760 Watt tungsten-halogen lamp.

3. Results

Luminescence spectra were recorded at 5 K and 2 K. Both the compensated and uncompensated crystals exhibit two widely separated regions of luminescence: one centred in the far red around 14065 cm^{-1} (711 nm), and the other in the near-IR around 8960 cm^{-1} (1116 nm). For the uncompensated crystal, each region exhibits some luminescence bands that show large variations in intensity as the crystal is cooled from about 5 K to 2 K. These bands are due to emission from a thermally equilibrated manifold of close-lying excited states formed by exchange coupling in Mo^{3+} dimers.

Luminescence in the far red has been shown [2] to arise from the $^2T_2 \rightarrow {}^4A_2$ relaxation of isolated Mo^{3+} centres and the corresponding $^2T_2\,{}^4A_2 \rightarrow {}^4A_2\,{}^4A_2$ transition of the pair-centres. The notation used is for O_h symmetry; the actual coordination

symmetry of a single Mo^{3+} ion and a Mo^{3+}–V–Mo^{3+} pair centre is D_{3d}. The near-IR luminescence is due to transitions from the lower energy ^2E single-ion and $^2E\,^4A_2$ pair centres. In principle, information concerning the ground state exchange splitting can be obtained from analysis of either system. In practice, the resolution and complexity of the two luminescence systems are markedly different due to differences in the excited state manifolds. The best analysis for the ground state dimer interaction has been obtained from analysis the $^2E\,^4A_2 \rightarrow {}^4A_2\,^4A_2$ luminescence.

Band positions and assignments are given in tables 1 and 2. Since all transitions are between ground and excited state manifolds, the 'origin' for purposes of measuring band positions is taken as the most intense inter-manifold transition, unless otherwise noted. In some cases, vibrational assignments have been made with reference to vibrational modes observed in the absorption spectrum of $Cs_3Mo_2Cl_9$ [7]. This lattice contains adjacent molybdenum ions with bridging and terminal chloride ligands in an approximate D_{3h} geometry. There is also a close corespondence between the terminal metal-chloride vibrational frequencies observed in $Cs_3Mo_2Cl_9$ and those seen in the spectra of Mo^{3+} dimers in $CsMgCl_3$. The absence of bridging metal-chloride vibrations is in agreement with the proposed structure of the dimer centre (figure 1).

3.1. The $^2T_2$ system

The principle luminescence band of the lithium-compensated lattice ClMoLi is a narrow peak at 14 167 cm^{-1}; this is taken to be the vibronic origin of the $^2T_2 \rightarrow {}^4A_2$ transition of an isolated Mo^{3+}–Li^+ centre. (See table 1.) The band is coincident, within experimental error of about ± 3 cm^{-1}, with a weak band in the absorption spectrum. Assignments for the absorption and luminescence spectra of the ClMoLi sample are given in table 1. The ClMoLi luminescence spectrum shows no evidence of exchange coupling (i.e. temperature sensitivity or fine structure). Since this material is fully compensated by the 15-fold excess of lithium, dimer formation is *completely* suppressed. It is probable, however, that the high lithium content creates a variety of minority defects in which lithium also replaces inter-chain cesium ions in various combinations. In fact, at least three very weak luminescence bands to higher energy at +19, +82, +106 cm^{-1} are due to minority sites.

The far red luminescence of the uncompensated lattice ClMo shown in figure 2 differs markedly from that of the compensated lattice ClMoLi. A strong, temperature-dependent peak at 14 066 cm^{-1} is taken as the origin of the $^2T_2\,^4A_2 \rightarrow {}^4A_2\,^4A_2$ dimer transition. The spectrum is dramatically temperature-sensitive between 2 and 5 K as illustrated in figure 2, suggesting that it arises from a manifold of closely spaced Mo^{3+} pair levels. At least 11 much weaker luminescence bands are observed between −7 and −323 cm^{-1} to lower energy of the origin; not all of these are shown in figure 2. The band assignments are given in table 2.

The corresponding ClMo absorption spectrum consists of the origin and five bands to higher energy—see table 2. Their assignment as vibronic bands is based upon comparison with vibrational intervals observed in the related compound $Cs_3Mo_2Cl_9$ [7].

3.2. The ^2E system

The spectra in the near-IR arise from the $^2E \rightarrow {}^4A_2$ transition of isolated Mo^{3+} centres and the $^2E\,^4A_2 \rightarrow {}^4A_2\,^4A_2$ transitions of dimer-pair centres. These spectra are more readily analysed than the far red $^2T_2$ spectra. The isolated centre emission is easily identified by comparison with the luminescence from the fully compensated

Table 1. Assignments for $CsMgCl_3$: Mo^{3+}: Li^+.

Frequency[a] (cm^{-1})	Intensity[b]		Assignment[c]
14273	m	$0' + 106$	$^2T_2 \rightarrow {}^4A_2$ (minority)
14249	m	$0' + 82$	$^2T_2 \rightarrow {}^4A_2$ (minority)
14186	m	$0' + 19$	$^2T_2 \rightarrow {}^4A_2$ (minority)
(14170)	w	$(0' - 0')$	$^2T_2 \rightarrow {}^4A_2$
14167	s	$0' - 0'$	$^2T_2 \rightarrow {}^4A_2$
14128	w	$0' - 39$	ν_1 [40]
14112	w	$0' - 55$	
14086	w	$0' - 81$	
14044	m	$0' - 123$	
14019	w	$0' - 148$	
14004	m	$0' - 163$	ν_3 [165]
13959	w	$0' - 208$	
13919	w	$0' - 248$	ν_4 [248]
13862	w	$0' - 305$	ν_5 [306]
13843	w	$0' - 324$	ν_6 [326]
8686.7	s	$0' - 300$[d]	$^2E \rightarrow {}^4A_2$
8659.1	w; broad	$0' - 300 - 27.6$	

[a] Frequencies in brackets are absorption bands.
[b] s = strong, m = medium, w = weak.
[c] Primed denotes monomer transition; unprimed denotes dimer transition; square brackets denote internal frequencies which consistently occur throughout the spectra; 'minority' refers to molybdenum monomer sites with slightly different local environments.
[d] Assignment as a vibronic origin is based on observation in reference [1] and unpublished results from the corresponding bromides.

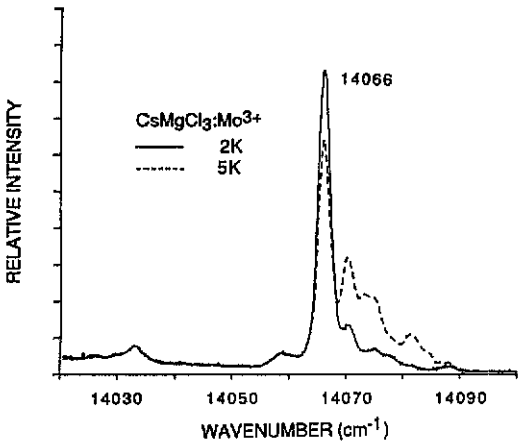

Figure 2. Luminescence spectra of $CsMgCl_3$:Mo^{3+} at 5 K and 2 K from the $^2T_2 {}^4A_2$ excited state.

Table 2. Assignments for $CsMgCl_3$: Mo^{3+}.

Frequency[a] (cm^{-1})	Intensity[b]		Assignment[c]
(14404)	w	(0 + 347)	a_{1g} M–Cl terminal stretch (350)
(14278)	m	(0 + 221)	a_{1g} M–Cl terminal bend (217)
(14241)	m	(0 + 184)	e_{2g} M–Cl terminal deformation (183)
(14117)	s	(0 + 60)	e_{2g} (55)
(14094)	s	(0 + 37)	e_{1g} (38)
14088	w	0 + 22	
14082	w	0 + 16	
14081	w	0 + 15	
14074	w	0 + 8	
14070	m	0 + 4	
14066	s	0 – 0	$^2T_2{}^4A_2 \rightarrow {}^4A_2{}^4A_2$
14059	w	0 – 7	
(14057)	m	(0 – 0)	$^2T_2{}^4A_2 \leftarrow {}^2T_2{}^4A_2$
14033	w	0 – 33	
14026	w	0 – 40	ν_1 [40]
14019	w	0 – 47	
13978	w	0 – 88	
13925	m	0 – 141	ν_2 [141]
13901	w	0 – 165	ν_3 [165]
13818	w	0 – 248	ν_4 [248]
13807	w	0 – 259	
13760	m	0 – 306	ν_5 [306]
13743	w	0 – 323	ν_6 [323]
8966.2	m	0 – 0	$^2E\,{}^4A_2 \rightarrow {}^4A_2{}^4A_2$
8963.7	s	0 – 2.5	
8958.0	m	0 – 8.2	
8955.5	m	0 – 10.7	
8950.6	m	0 – 15.6	
8949.8	m	0 – 16.4	
8947.0	w	0 – 19.2	
8933.0	w	0 – 33.2	
8825.0	w	0 – 141	
8815.7	w	0 – 150	ν_2 [141]
8807.9	w	0 – 158	
8787.5	w	0 – 179	
8779.6	w	0 – 217	
8735.8	w	0 – 230	
8699.1	w	0 – 267	
8685.9	w	0 – 280	
8658.9	w	0 – 307	ν_5 [306]
8639.9	w	0 – 326	ν_6 [326]

[a] Frequencies in brackets are absorption bands.
[b] s = strong, m = medium, w = weak.
[c] Primed denotes monomer transition; unprimed denotes dimer transition; square brackets denote internal frequencies which consistently occur throughout the spectra; vibrational symmetry assignments are from reference [7].

crystal ClMoLi. At 5 K and 2 K the crystal shows a single sharp luminescence peak at 8686.7 cm^{-1} that is assigned as the vibronic origin of the $^2E \rightarrow {}^4A_2$ emission (table 1). The luminescence spectrum of the uncompensated crystal ClMo shown in figure 3 exhibits a set of sharp bands centred at 8960 cm^{-1} and spanning about 19 cm^{-1} (see table 2). These bands are very temperature-sensitive between 5 K and 2 K, and are attributed to exchange-coupled Mo^{3+} ions.

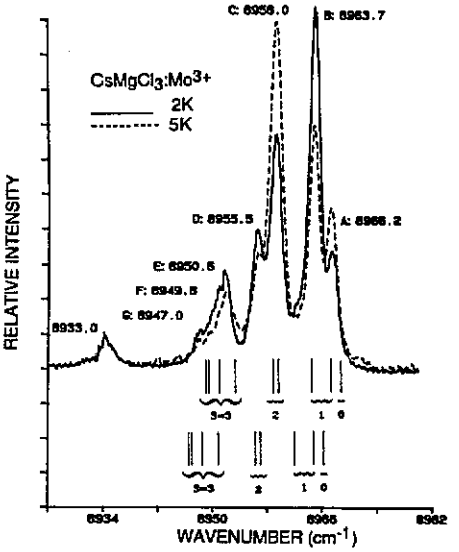

Figure 3. Luminescence spectra of Mo^{3+} pairs in $CsMgCl_3$:Mo^{3+} at 5 K and 2 K from the $^2E\,{}^4A_2$ excited state. The ground state energy levels were calculated from the reported EPR parameters [4]. The two sets are separated by 2.5 cm^{-1}. The letters correlate with the transitions shown in figure 4.

4. Discussion

The symmetry of the Mo^{3+}–V–Mo^{3+} group together with the associated halogens is D_{3d}. The $^4A_2{}^4A_2$ ground state of the exchange-coupled Mo^{3+} ions yields a ground state multiplet with states of total spin $S = 0, 1, 2, 3$. The four resulting terms are $^1A_{1g}$, $^3A_{2u}$, $^5A_{1g}$, and $^7A_{2u}$. The splitting of these multiplet components can be described by a phenomenological Hamiltonian for the magnetic coupling between two Mo^{3+} ions α and β. The Hamiltonian includes the isolated ion Hamiltonians H_α and H_β and terms for isotropic (J) and axially symmetric exchange coupling (D_e). The isolated MO^{3+} Hamiltonian is given by

$$H_\alpha = H_\beta = S \cdot D_c \cdot S \tag{1}$$

where D_c is the isolated ion axial zero field splitting parameter. The dimer Hamiltonian is then,

$$H = H_\alpha + H_\beta + JS_\alpha S_\beta + S_\alpha D_e S_\beta \,. \tag{2}$$

The spin function basis for the coupled pair is constructed from the 16 single ion functions $|S_\alpha, m_\alpha\rangle|S_\beta, m_\beta\rangle$ for $S_\alpha = S_\beta = 3/2$.

Analysis of the EPR spectra has indicated that the dimer coupling is antiferromagnetic in the ground state, and so the $S = 0$ state lies lowest in energy [4]. The ground state multiplet splitting (figure 4) has been determined by iterative adjustment of the spin-Hamiltonian parameters to obtain the best fit to the ground state EPR spectrum. The analysis indicates that the isotropic exchange interaction is of the same order of magnitude as the zero-field splitting: $J = 2.75$ cm^{-1}, $D_e = -0.0033$ cm^{-1}, $D_c = -1.139$ cm^{-1}.

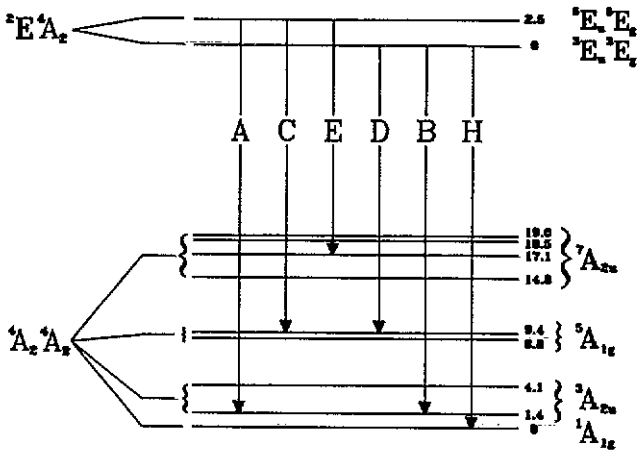

Figure 4. A schematic energy level diagram for Mo^{3+} pair centres. Ground state splittings were calculated from EPR Hamiltonian parameters [4].

The luminescence spectrum terminating on the levels of the $^4A_2{}^4A_2$ ground state multiplet should reveal the multiplet splitting. However, analysis of the luminescence spectrum is complicated by the fact that more than a single excited state multiplet component is thermally populated, so that the structure of the luminescence spectrum depends upon both the ground and excited state multiplet splitting.

The first excited state of the exchange-coupled ions, $^2E\,{}^4A_2$, is a complex manifold containing the states ^3E_g, ^3E_u, ^5E_g and ^5E_u. Under spin–orbit coupling each triplet state yields $A_1 + A_2 + 2E$ and each quintet state yields $2A_1 + 2A_2 + 3E$, each with the proper parity label. In a strongly coupled Cr^{3+} dimer Riesen and Güdel [8] found that the two triplet states lie lower in energy and the spinor levels of these two excited states spanned only about 30 cm^{-1}. The Cr^{3+} dimer coupling is considerably stronger than that of the Mo^{3+} dimers in $CsMgCl_3$. A much smaller splitting within the $\{^3E_g\,{}^3E_u\}$ and $\{^5E_g\,{}^5E_u\}$ excited state manifolds is expected for the more weakly coupled Mo^{3+} dimers.

Considering both the excited state and ground state multiplet splitting, the spectral envelope of the dimer luminescence may be written

$$I(v) = N'Z^{-1} \sum_{i,j} \exp(-E_i/kT) \cdot k_{ij} \tag{3}$$

where $I(v)$ is the luminescene intensity with maxima at $v = (E_{00} + E_i - E_j)/h$. E_{00} is the energy separation of the lowest energy components of the ground and excited states. The indices i and j run over excited state and ground state multiplet components, respectively. The energies E_i and E_j are relative to the lowest multiplet component. N' is the population of the excited state manifold and Z is a suitable partition function for the multiplet manifolds and k_{ij} is the transition probability between the i^{th} and j^{th} multiplet components.

If, at the lowest temperatures attained, only a single excited state manifold level is populated, then the spectrum is determined entirely by summation over the ground state manifold:

$$I(v) = N'Z^{-1}\sum_{0,j} k_{0j} \tag{4}$$

and bands are observed at the frequencies $v = (E_{00} - E_j)/h$ determined by the ground state multiplet energies E_j.

At elevated temperatures, population of higher excited state manifold levels will produce luminescence bands shifted to higher energy at frequencies $v = (E_{00} - E_j)/h$ with intensities given by (3).

4.1. The $^2E\,^4A_2$ system

The near-IR luminescence of the ClMo sample (figure 3) may be analysed by assuming that emission arises principally from two states or clusters of states ($i = 0, 1$) in the $^2E\,^4A_2$ multiplet. If we assume as a first approximation that transitions to all components of the ground state are allowed, luminescence will produce the effect of two superimposed spectra whose relative positions reflect the excited state component separation. From both the relative displacement and the temperature dependence of the superimposed spectra, the excited state separation is inferred to be 2.5 cm^{-1}.

Using the 2.5 cm^{-1} excited state component separation, the 16 eigenvalues (several of which are degenerate) of the dimer Hamiltonian are correlated with the luminescence of ClMo in figure 3. The band positions of the superimposed spectra are in agreement with the ground state multiplet splittings shown in figure 3 by the vertical lines. The spin–orbit and crystal field splitting predicted by the spin-Hamiltonian analysis are fairly well, but not completely resolved in the optical spectrum.

The optically observed 8.2 cm^{-1} energy separation between the 'hot' bands (A and C) and the corresponding 'cold' bands (B and D) matches well with the recorded 8.0 cm^{-1} EPR splitings between one of the $^5A_{1g}$ and one of the $^3A_{2u}$ ground state levels. This observation suggests that transitions A and B terminate on the $^3A_{2u}$ ground state level, while C and D terminate on the $^5A_{1g}$ ground state level as suggested in figure 4.

A hypothetical energy level diagram (figure 4) for the $^2E\,^4A_2 \rightarrow {}^4A_2\,{}^4A_2$ transition may be drawn using the observed 2.5 cm^{-1} excited state manifold separation, the EPR ground state splitting and the electric dipole selection rules $g \leftrightarrow u$ and $\Delta S = 0, \pm 1$. The proposed $^2E\,^4A_2 \rightarrow {}^4A_2\,{}^4A_2$ energy level diagram correctly predicts the relative spacing, temperature dependence and intensity ordering for the four strongest transitions (A, B, C, D). Furthermore, it also predicts that transitions B and C, for which $\Delta S = 0$, should be the strongest bands. Transition H shown in figure 4 is not seen. It is expected to be weaker since it involves the $\Delta S = 1$ selection rule. It is also expected to lie close to band A and may lie in the envelope of this band.

The weaker transitions E, F and G can also be predicted from the above energy level diagram if electric dipole selection rules are relaxed. This is a reasonable assumption since, when spin–orbit coupling is included, group theoretical considerations indicate that each excited state spinor can emit to some ground state spinor of opposite parity, with the exception of the A_{2g}–A_{2u} and A_{1g}–A_{1u} combinations.

Although the proposed energy level diagram is preliminary, it does predict the relative intensities, spacing and temperatue dependence of the $^2E\,^4A_2 \rightarrow {}^4A_2\,{}^4A_2$ near-IR emission. This agreement with the experimental data suggests that such an energy level diagram is at least a fair representation of the observed Mo dimer $^2E\,^4A_2 \rightarrow {}^4A_2\,{}^4A_2$ luminescence.

4.2. The $^2T_2\,^4A_2$ system

Temperature-dependent behaviour is observed for the far red luminescence of ClMo (figure 2). The luminescence bands in this region roughly correspond to the ground state manifolds calcualted from EPR spectroscopy. While the energy range spanned is less clear than in the 8960 cm^{-1} region. This is to be expected due to the greater density of emitting states in the $^2T_2\,^4A_2$ multiplet. The number of superimposed spectra is greater and the complexity of the resulting spectrum makes analysis difficult.

5. Conculsions

The addition of Mo^{3+} together with Li^+ to $CsMgCl_3$ results in crystals containing only spatially isolated Mo^{3+} ions. Neither the EPR spectra nor the luminescence spectra provide any evidence of pair formation. The addition of Mo^{3+} alone to this lattice, on the other hand, results in pair formation of the type Mo^{3+}–V–Mo^{3+}. The spectra show no single ion features, but only absorption due to pairs.

The near-IR luminescence of the ClMo sample at 5 K has been analysed in terms of two superimposed spectra each originating from a different component in the $^2E\,^4A_2$ excited state. This scheme along with the proposed $^2E\,^4A_2 \rightarrow {}^4A_2\,{}^4A_2$ energy level diagram models fairly well the observed luminescence.

References

[1] Flint C D and Paulusz A G 1981 *Mol. Phys.* **44** 925
[2] Vanoy T C and McPherson G L 1988 *Chem. Phys. Lett.* **143** 51
[3] McPherson G L, McPherson A M and Atwood J L 1980 *J. Phys. Chem. Solids* **41** 495
[4] McPherson G L, Varga J A and Nodine M H 1979 *Inorg. Chem.* **18** 2189
[5] McPherson G L and Henling L M 1977 *Phys. Rev.* B **16** 1889
[6] McPherson G L, Heung W and Barraza J J 1978 *J. Am. Chem. Soc.* **100** 469
[7] Smith P W and Stranger R 1986 *Aust. J. Chem.* **39** 1269
[8] Riesen H and Güdel H U 1987 *Mol. Phys.* **60** 1221